

Sediment trapping by a tree belt: processes and consequences for sediment delivery

Sophie Legu dois, Tim Ellis, Peter Hairsine, David Tongway

► **To cite this version:**

Sophie Legu dois, Tim Ellis, Peter Hairsine, David Tongway. Sediment trapping by a tree belt: processes and consequences for sediment delivery. *Hydrological Processes*, Wiley, 2008, 22 (17), pp.3523-3534. 10.1002/hyp.6957. hal-02659353

HAL Id: hal-02659353

<https://hal.inrae.fr/hal-02659353>

Submitted on 30 May 2020

HAL is a multi-disciplinary open access archive for the deposit and dissemination of scientific research documents, whether they are published or not. The documents may come from teaching and research institutions in France or abroad, or from public or private research centers.

L'archive ouverte pluridisciplinaire **HAL**, est destin e au d p t et   la diffusion de documents scientifiques de niveau recherche, publi s ou non,  manant des  tablissements d'enseignement et de recherche fran ais ou  trangers, des laboratoires publics ou priv s.

Sediment trapping by a tree belt: processes and consequences for sediment delivery

Sophie LEGUÉDOIS* Tim W. ELLIS[†] Peter B. HAIRSINE[‡]
David J. TONGWAY[§]

October 21, 2007

*Corresponding author. INRA, UR272 – Science du sol, BP 20619, F-45166 Olivet, France.
Presently at Laboratoire d'écologie fonctionnelle (EcoLab) – UMR 5245 CNRS / Université Paul Sabatier / INP-ENSAT, BP 32607, F-31326 Castanet-Tolosan, France. Phone: +33 (0)5 62 19 39 00. Fax: +33 (0)5 62 19 39 01. Email: sophie.leguedois@ensat.fr

[†]CSIRO Land and Water, GPO Box 1666, Canberra ACT 2601, Australia. Phone: +61 (0)2 6246 5743.
Email: tim.ellis@csiro.au

[‡]CSIRO Land and Water, GPO Box 1666, Canberra ACT 2601, Australia. Phone: +61 (0)2 6246 5924.
Email: peter.hairsine@csiro.au

[§]CSIRO Sustainable Ecosystems, GPO Box 284, Canberra City ACT 2601, Australia. Phone: +61 (0)419 861 615. Email: david.tongway@csiro.au

ABSTRACT

Restoring belts of perennial vegetation in landscapes is widely recognised as a measure to improving landscape function. While there have been many studies of the transport of pollutants through grass filter strips, few have addressed sediment related processes through restored tree belts. In order to identify these processes and to quantify their relative contribution to sediment trapping, a series of rainfall simulations was conducted on a 600-m² hillslope comprising a pasture upslope of a 15-year-old tree belt. Although the simulated events were extreme (average recurrence intervals ~ 10 and 50 y), the trapping efficiency of the tree belt was very high: at least 94 % of the total mass of sediments was captured. All the size fractions were trapped with a minimum Sediment Trapping Ratio (STR) of 91 % for the medium-sized fragments. Fractions < 1.3 µm and > 182 µm were totally captured (STR=100 %). Through the joint analysis of sediment budgets and soil surface conditions, we identified different trapping processes. The main trapping process is the sedimentation (at least 62 % of trapped sediment mass) with deposits in the backwater and as micro-terraces within the tree belt. Modelling results show that the coarsest size fractions, above 75 µm are preferentially deposited. Joint infiltration of water and sediments has also been noticed however this process cannot explain alone the selective trapping of the finest fractions. We suggest that the finest fractions transported by the overland flow may be trapped by adsorption on the abundant litter present within the tree belt.

Keywords: runoff, size selectivity, sediment delivery, tree litter, backwater, sedimentation, macropores

Abbreviations

ASD Aggregate Size Distribution

COF Coarse Organic Fragments

- 1 **MSF** Mineral Soil Fragments
- 2 **MWD** Mean Weight Diameter
- 3 **P** Pasture, referring to the pasture plot
- 4 **P+TB** Pasture + Tree Belt, referring to the pasture + tree belt plot
- 5 **RMSE** Root Mean Square Error
- 6 **TB** Tree Belt, referring to the tree belt plot
- 7 **VFS** Vegetative Filter Strip

8 **Introduction**

9 Managed rows of trees or shrubs are common features in agricultural landscapes through-
10 out the world ([Baudry et al., 2000](#)). They have been promoted as a measure for a wide
11 range of benefits and functions related to water management, soil conservation, biodiver-
12 sity or farming production (e.g. see [Kang et al., 1990](#); [Baudry et al., 2000](#); [Stirzaker et al.,](#)
13 [2002](#); [Droppelmann and Berliner, 2003](#)). When located between agricultural land and
14 waterbodies in the form of tree belts, they can be used as a Vegetative Filter Strip (VFS)
15 to trap agricultural diffuse pollution transported by overland flow and, consequently to
16 improve the quality of surface water.

17 Sediments, which are generated by water erosion on agricultural lands, are one form of
18 diffuse agricultural pollution that impairs water quality by increasing the turbidity and the
19 delivery of particle-bound chemicals. VFSs have been shown to present a high trapping
20 capacity and to be an effective tool to control sediments from agricultural lands (e.g.
21 see the reviews by [Dosskey, 2001](#); [Helmets et al., 2005](#)). However most of the studies
22 concern grass strips ([Dosskey, 2001](#)) or tree and shrub strips implemented downslope of
23 a grass strip ([Daniels and Gilliam, 1996](#); [Schmitt et al., 1999](#); [Sheridan et al., 1999](#); [Lee](#)

1 et al., 2000) and few studies (Cooper et al., 1987; Hairsine, 1996; Loch et al., 1999) have
2 focussed on sediment trapping by tree belts alone.

3 A range of different processes act within VFS to trap sediments (Dosskey, 2001).
4 Sedimentation is the best known trapping process. It occurs when the flow velocity is
5 retarded by the VFS and, consequently, the sediment transport capacity decreases. Most
6 of the time, sedimentation happens in the ponding areas, called backwater, that formed
7 upstream of the VFS (Dillaha et al., 1988; Dabney et al., 1995; Meyer et al., 1995; Ghadiri
8 et al., 2001). Deposits can also be found within the VFS itself (Dillaha et al., 1988).
9 Sedimentation can be enhanced by the loss in runoff discharge due to the high infiltration
10 capacity in the strip (Hayes et al., 1984; Lee et al., 1989). The removal of particles in
11 surface runoff, with the infiltration of water, has also been evoked as another possible
12 trapping process (Lee et al., 2000; Dosskey, 2001).

13 In most of the work on sediment trapping in VFSs, the buffer zone is considered as a
14 black box and the specific impact of the various trapping processes are not examined (e.g.
15 see Hayes et al., 1984; van Dijk et al., 1996; Muñoz-Carpena et al., 1999; Lee et al., 2000;
16 Le Bissonnais et al., 2004). Trapping processes, especially backwater sedimentation,
17 have been analysed in detail in laboratory studies with disturbed soils (Dabney et al.,
18 1995; Meyer et al., 1995) or flume beds (Jin and Römken, 2001; Ghadiri et al., 2001; Jin
19 et al., 2002) and, consequently, are not representative of field conditions. If knowledge
20 on sediment trapping processes is scarce for VFS in general, it is lacking for tree belts in
21 particular.

22 Movement of material on the soil surface leaves characteristic visual features, like de-
23 posits or sealing, which can be used to track the processes (Auzet et al., 1993; Tongway
24 and Hindley, 2004; van Dijk et al., 2005). The monitoring of the soil surface conditions
25 can be used as a rapid tool to obtain information on the trapping processes acting within
26 a VFS. Trapping can also change the size distribution of the flux of sediments. For ex-
27 ample, the coarsest size fractions are selectively deposited over an area of sedimentation
28 (Beuselinck et al., 1999b). So, information on the processes acting within a VFS can be

1 obtained by analysing the size distribution of sediments entering and leaving the buffer
2 zone.

3 The objectives of the work presented in this paper are (i) to identify the trapping pro-
4 cesses within a tree belt and (ii) to assess their relative contribution to the total sediment
5 trapping, by analysing changes in soil surface conditions, as well as input and output sus-
6 pended sediment size distribution. A field experiment was performed in order to have
7 realistic soil conditions. The hydrological aspect of this work is reported by [Ellis et al.](#)
8 (2006).

9 **Materials and methods**

10 **Study site**

11 The experimental site was located on a grazing property near Boroowa (-34° 22' S 148° 42'-
12 E), New South Wales, Australia. The studied tree belt was aligned perpendicular to the
13 slope (6°) in the lower part of a hillslope covered with sheep pasture. The trees were di-
14 rectly seeded in 1990 mainly with *Acacia* spp. and *Calistemon* spp. so that the trees have
15 been established for 15 y at the time of the experiment. The tree belt was originally setup
16 by the landholder for stock shelter and biodiversity habitat. Stock were excluded from the
17 belt by a fence located near the drip line of the present canopy. The soil of the site is a
18 chromic luvisol ([Driessen et al., 2001](#)) with a silt loam surface horizon.

19 **Experimental layout**

20 The experiment was conducted on a $15 \times 40 \text{ m}^2$ area which comprised $15 \times 28 \text{ m}^2$ of
21 grazed pasture draining into $15 \times 12 \text{ m}^2$ of tree belt (Fig. 1). The experimental area was
22 divided into three plots (Fig. 1) in order to assess the behaviour of respectively: (i) the
23 whole system (plot P+TB), i.e. pasture draining into the tree belt; (ii) the pasture itself
24 (plot P); (iii) and the tree belt itself (plot TB). The plots edges were formed by strips of

1 sheet steel, embedded in the soil ~ 40 mm and sealed at soil level with liquid petroleum
2 jelly. At each plot outlet the runoff water and sediment were collected in a gently inclined
3 (2°) steel trough and then directed into a portable ‘RBC’ flume (Bos et al., 1991) .

4 In order to have two similar pasture-tree belt sequences, we located the experimental
5 area on a part of the study site with uniform slope, soil conditions, as well as pasture and
6 tree covers. Ellis et al. (2006) demonstrated, with two analytical checks, that any likely
7 error in the surface water budget due to spatial variation between the sequences was likely
8 to be smaller than the measurement errors. This choice of experimental configuration
9 was necessary to allow sequences comparison. However it artificially favoured sheet
10 flow whereas flow concentration, which is likely to occur on farm, was shown to impair
11 sediment trapping (Dillaha et al., 1989; Dosskey, 2002).

12 **Rainfall simulation**

13 Rainfall was applied on the whole 600 m² experimental plot using a large portable rainfall
14 simulator. Details on the setup of this rainfall simulator are given in Wilson (1999).
15 Twenty risers which support the nozzles were arranged on the plot in a triangular pattern,
16 with 6 m between each riser (Fig. 1). The risers were 3 m high in the pasture and 7 m
17 high, above the tree tops, in the tree belt. The setting of the sprinklers above the tree tops
18 ensured to reproduce rainfall interception by the canopy. Even if the rainfalls were quite
19 variable over the experimental area (see standard deviation values in Table 1) the rainfall
20 homogeneity between the plots was good (Table 1) as weather conditions were windless
21 at the time of the experiments.

22 Three simulated rainfall events were successively applied over the experimental area
23 (Table 1): a pre-wetting event at medium intensity to ensure an initial wet soil surface, and
24 two longer run events at medium and high intensity. Time constraints required that rainfall
25 events were applied sequentially within ~ 30 min of each other. These rainfall events are
26 quite exceptional for the region of Boorowa with important Average Recurrence Intervals
27 (ARI, see Table 1), i.e. the average, or expected, value of the periods between exceedances

1 of a given rainfall total accumulated over a given duration. These intense rainfall events
2 enable us to test the tree belt trapping capacity for extreme conditions, i.e. concentrated
3 flow or exceptional rainstorm, when it is expected that much of the long term flux of
4 sediment occurs.

5 **Measurements and sampling**

6 Flow depths were measured manually at 3 min intervals using a ruler in portable ‘RBC’
7 flumes (Bos et al., 1991). Depths were converted to discharge rates using the relationship
8 provided by Bos et al. (1991).

9 At each sampling site, two overland flow samples were taken every 3 min at the bottom
10 of the trough, just below the flume, during the runoff event, i.e. during the rainfall as well
11 as during the hydrograph recession period. The first set of samples was processed to
12 determine the sediment concentration. These runoff samples were first weighed for the
13 water and sediment mass, then oven-dried at 105°C and finally weighed again to obtain
14 the dry sediment mass.

15 The second set was used to determine aggregate size distribution (ASD) of the sed-
16 iments by combining sieving and laser diffraction analysis data. The ASD is the size
17 distribution, before dispersion, of the soil fragments, i.e. aggregates and primary parti-
18 cles, that make up the sediment phase. The analysis of this set was performed one week
19 after sampling. The samples were kept in a fridge at around 4 °C to avoid reaggregation
20 by biological activity. Before the laser diffraction measurement each sample was gently
21 wet sieved by hand. The first samples were sieved at 595 µm (sieve opening diameter)
22 but, for the following samples, we adapted our procedure and sieved at 1680 µm to use
23 the full size range of the laser diffraction sizer. In the following text, the general term
24 ‘undersize’ will be used to call both the < 595 and the < 1680 µm fractions. When the
25 concentration of the undersize suspension was too high for laser diffraction measurement,
26 the sample was split using a chute splitter after the sieving. In other samples, the sedi-
27 ment concentration was too low enough for laser diffraction analysis. This was the case

1 for the samples collected at the outlet of plot TB during event # 1. All the undersize sam-
 2 ples or sub-samples with a sufficiently high sediment concentration were analysed by a
 3 laser diffraction sizer (Malvern Mastersizer 2000) which gave the volume distribution of
 4 68 fractions (i.e. the maximum number of fractions available for this sizer) between 0.02
 5 to 2 000 μm . The limits of the fractions were set in order to logarithmically increase the
 6 size range with the diameter. As the laser diffraction sizer measures volume distribution,
 7 the ASDs were expressed in volume percentage. In case of sub-sampling, the measured
 8 size distributions S_{ij} of all the n sub-samples j for a given sample i were averaged by
 9 arithmetic mean:

$$10 \quad S_i = \frac{\sum_{j=1}^n S_{ij}}{n}. \quad (1)$$

11 The undersize and oversize fractions were then oven-dried (105 °C) and weighed in order
 12 to determine their relative proportion. To assess the impact of two diameter sieve sizes on
 13 size measurement, the ASDs of samples collected from the same event (event # 2) and plot
 14 (plot P+TB) were compared. As shown on Figure 2, the differences between the ASDs
 15 from these two groups are small. This figure indicates that even for the samples sieved at
 16 595 μm , the laser sizer detected a large proportion of particles coarser than 600 μm . This
 17 is due to the fact that the size parameter characterised by laser diffraction, i.e. volume
 18 diameter, and by sieving, i.e. sieve diameter, is different.

19 When a comparison of many size distributions was needed, the ASDs were sum-
 20 marised by their Mean Weight Diameter (MWD), i.e. the average diameter weighted by
 21 the proportion. In our case, the ASDs are volume distributions and, thus, the proportions
 22 are expressed as volume percentage:

$$23 \quad MWD = \frac{\sum^i p(i) \times \phi(i)}{\sum^i p(i)}, \quad (2)$$

24 where $p(i)$ and $\phi(i)$, are the volume percentage and the arithmetic mean size of a given
 25 size fraction i respectively.

1 For some samples taken during the steady state runoff phase, the settling velocity
 2 distribution was determined with the automated settling column proposed by Loch (2001)
 3 from a design of Hairsine and McTainsh (1986). The settling velocity distributions were
 4 expressed in mass percentage.

5 After drying, a subset of the oversize fractions was analysed for bulk density. De-
 6 pending on their shape, the constituents were divided into different categories. For each
 7 shape fraction j , the different necessary to determine the dry and the wet bulk densities
 8 were measured. The dry samples were weighed for dry mass, $m_d(j)$ (in g). The volume of
 9 each shape fraction, $v(j)$ (in cm^3), was determined on the dry samples by combining im-
 10 age acquisition with a flat bed scanner and image analysis with the software WinRHIZO
 11 © (Regent Instrument INC, 2005). For the fractions with round-shaped particles (mainly
 12 sticks and some spherical fruits), the software gave directly a volume estimate by assum-
 13 ing all the particles were cylindrical. For the fractions with flat-shaped particles, only the
 14 projected surface area was determined by image analysis and the average thickness was
 15 measured using vernier callipers. For wet mass ($m_w(j)$, in g) measurement, the shape frac-
 16 tions were wetted before weighing by soaking the samples for 1 h and then air-drying for
 17 1.5 h until no free water was present. None of the shape fractions showed a measurable
 18 swelling, so the volume of the wet samples was assumed to be the same as the volume of
 19 the dry samples. The dry bulk density, ρ_d ($\text{g}\cdot\text{cm}^{-3}$), and the wet bulk density, ρ_w ($\text{g}\cdot\text{cm}^{-3}$),
 20 were computed for the whole size fraction as mean weight densities:

$$21 \quad \rho_d = \frac{\sum^j \left(m_d(j) \times \frac{m_d(j)}{v(j)} \right)}{\sum^j m_d(j)} \text{ and} \quad (3)$$

22

$$23 \quad \rho_w = \frac{\sum^j \left(m_w(j) \times \frac{m_w(j)}{v(j)} \right)}{\sum^j m_w(j)}. \quad (4)$$

1 Spatial and temporal changes in overland flow and associated changes in soil surface
 2 conditions were recorded during all the rainfall events. Before and after each rainfall
 3 event, the soil surface condition was assessed along 4 transects of the experimental area
 4 following the method of [Tongway and Hindley \(2004\)](#). This careful visual assessment of
 5 the soil surface evolution gave useful evidences to aid in the interpretation of measured
 6 sediment movement.

7 **Data computation**

8 The total mass of soil leaving a given experimental plot j and for a given runoff event, M_j
 9 (kg), was computed by piecewise integration of the equation:

$$10 \quad M_j = \int_{t_i}^{t_e} (q_j(t) \times c_j(t)) dt, \quad (5)$$

11 where t_i the time to incipient runoff, t_e the time that runoff ends, $q_j(t)$ the water discharge
 12 rate and $c_j(t)$ the sediment concentration. $q_j(t)$ and $c_j(t)$ were determined by linear inter-
 13 polation from discrete measurements of water discharge rates and sediment concentration
 14 respectively, at the outlet of plot j .

15 The mass of sediments produced by the pasture and delivered to the upper limit of
 16 the tree belt, Q_{input} (kg), can either be trapped by or pass through the tree belt. At the
 17 outlet, the total mass of sediments, Q_{output} (kg), contains only sediments which passed
 18 through the tree belt as well as sediments that were produced within the tree belt. As a
 19 consequence, the total net mass of sediments trapped within the tree belt equals:

$$20 \quad Q_{\text{trap}} = Q_{\text{input}} - Q_{\text{output}} + Q_{\text{TB}}, \quad (6)$$

21 where Q_{TB} (kg) is the mass of sediments produced within the tree belt. Q_{input} , Q_{output} and
 22 Q_{TB} were assessed by the measurements made at the outlets of plot P, plot P+TB, and plot
 23 TB, respectively.

24 The sediment budget for the tree belt compartment was estimated by a Sediment Trap-

1 ping Ratio, defined as STR:

$$2 \quad \text{STR} = \frac{Q_{\text{trap}}}{Q_{\text{input}}} = \frac{M_{\text{P}} - M_{\text{P+TB}} + M_{\text{TB}}}{M_{\text{P}}}, \quad (7)$$

3 where M_{P} , $M_{\text{P+TB}}$ and M_{TB} , are the total masses of sediment collected at the outlets of
4 plots P, P+TB, and TB, respectively. The STR is related to the more classically used Sed-
5 iment Delivery Ratio SDR (e.g. [Beuselinck et al., 1999a](#); [Muñoz-Carpena and Parsons,](#)
6 [2004](#)) by the following equation:

$$7 \quad \text{SDR} = 1 - \text{STR}. \quad (8)$$

8 **Results**

9 **Runoff characteristics and capture**

10 [Ellis et al. \(2006\)](#) provide a detailed analysis of the surface hydrology. Only a brief
11 summary is presented here. The runoff generation within the pasture was mainly governed
12 by a bare and crusted zone in the 3.5-m area upslope of the tree belt (see Figure 1). The
13 absence of vegetation in this zone is probably due to tree-pasture competition for soil
14 water and animal activities such as grazing, trampling and camping in the shade. The
15 specific discharges measured at the outlet of plot P during the steady state period reached
16 0.134 ± 0.005 and $0.298 \pm 0.009 \text{ l}\cdot\text{s}^{-1}\cdot\text{m}^{-1}$ (average \pm standard error) for event # 1 and
17 event # 2, respectively. [Ellis et al. \(2006\)](#) showed that 32 to 68 % and 0 to 28 % of the
18 runoff volume produced by the pasture was captured by the tree belt during events # 1
19 and 2, respectively. By analysing the hydrographs, they also show that the hydraulic
20 parameters of overland flow were greatly affected by the tree belt (Table 2). For both
21 rainfall events, the tree belt systematically showed a higher hydraulic roughness as well
22 as a deeper and slower flow. As a consequence, an area of ponded water, or backwater,
23 formed in the pasture just upslope of the tree belt.

1 **Evolution of the soil surface conditions in the tree belt**

2 Within the tree belt the initial soil surface conditions consisted of a dense tree litter on
3 approximately 83 % of the experimental area, while a sparse tree litter existed on the
4 remaining area. The litter was made of narrow, interlocking foliage as well as fine twigs.
5 When the overland flow, produced by the pasture area in plot P+TB, reached the tree belt,
6 it removed the litter fragments and rearranged them in small litter dams up to 25 mm high
7 and approximately 100 mm apart (Figure 3). These litter dams started to form during the
8 pre-wetting event. This surface condition remained present throughout the experiment.
9 During the rainfall events, the litter dams slowed the flow and led to the formation of small
10 ponds just upstream of each of them. Once the rainfall stopped, the ponds emptied. The
11 deposition of sediment in these ponds created micro-terraces (Figure 3). The formation
12 of the litter dams took place in the whole tree belt but micro-terraces development mainly
13 occurred in the first 1.5 m of the belt area. Both processes were active during all rainfall
14 events. The micro-terraces were no more than 1-mm-thick, with a maximum thickness
15 located in the concentrated flow paths that appeared during event # 1. The same processes,
16 litter dam building and micro-terrace formation, were also apparent in plot TB. However
17 these processes were far less intense in this plot since no overland flow entered from the
18 pasture.

19 Another soil surface feature which changed during the rainfall events was the presence
20 of macropore openings at the soil surface. Before rainfall simulations, the tree belt soil
21 contained 5-to-10-mm diameter macropores which were open at the surface. They were
22 mostly found beneath the tree litter within the first 1 to 2 m of the tree belt. Some of
23 them were tagged at the beginning of the rainfall. After event # 1, they were filled with
24 sediment.

25 During the two rainfall events, on plot P+TB, water ponded just upslope from the tree
26 belt, right at the interface of the pasture and the tree belt areas. The formation of the
27 backwater was accentuated, during the pre-wetting event, by the development of a litter
28 barrier due to the washing of plant debris that was initially located in the bare soil zone.

1 The ponded water led to the deposition of a triangular-shaped wedge of sediment with the
2 maximum depth (1.2 cm) just upstream from the litter barrier. This deposit, situated along
3 the whole length of the pasture-tree belt interface, was about 60 cm wide. Considering
4 a bulk density value of $1.4 \text{ g}\cdot\text{cm}^{-3}$, as measured by [Takken et al. \(1999\)](#), we computed
5 that $\sim 38 \text{ kg}$ of sediments accumulated at this location during the pre-wetting phase and
6 the two rainfall events. This corresponds to an average mass per unit width of tree belt of
7 $5.1 \text{ kg}\cdot\text{m}^{-1}$. In plot P, no ponded area formed and no backwater deposition was observed
8 upstream of the collection trough.

9 **Sediment size distributions**

10 MWD values were computed from the ASDs determined by laser diffraction method.
11 These values allowed determination of the temporal evolution of the size distribution dur-
12 ing rainfall events. The results ([Figure 4](#)), show that the MWD values are quite steady for
13 a given sample set. The only noticeable change in the MWD is the sharp increase after
14 rainfall has ceased for the two series collected at the outlet of plot P. So, the sediment
15 size distribution leaving the different hillslope plots seems to stay constant during rainfall
16 simulation. Once the rainfall had ceased and the runoff rate decreased, the sediments that
17 had left the pasture plot tended to get coarser.

18 The average sediment size distributions that left the three hillslope plots during the
19 two events are shown in [Figure 5](#). Only samples collected during a rainfall event were
20 taken into account to compute these distributions, and the samples collected during the
21 recession period were excluded. No particles were detected in the coarsest size fraction
22 ranging between 1905 to 2108 μm .

23 For a given plot, the ASDs were very similar across rainfall events. The data show only
24 a small enrichment in the medium-size fraction for event # 2 as compared to event # 1.
25 This enrichment occurred in the fractions between 5 and 150 μm for the P+TB plot, and
26 the fractions between 30 and 150 μm for the P plot.

27 The sediments that moved from plot P had the finest ASD. The measured size range

1 is from 0.5 to 1900 μm . Sediments collected at the outlet of plot TB (data available only
2 for event # 2) were the coarsest, with a measured size range from 3 to 1900 μm and 92 %
3 of their volume made up of coarse-size fraction between 479 and 1660 μm . For plot
4 P+TB, the ASDs have a shape quite similar to the ASD measured from plot TB with a
5 higher proportion of medium sediment sizes (from around 8 to 150 μm). The sediments
6 from plots TB and P+TB mostly consisted of the 479 to 1660 μm size fraction which was
7 nearly 90 % and 84 % of the volume for event # 1 and event # 2, respectively. The high
8 contribution of the coarse-size fraction is the most distinctive characteristic of the ASDs
9 measured on these plots.

10 **Settling velocity distributions**

11 The three measurements of settling velocity distribution are given in Figure 6. The settling
12 velocity distributions of sediment particles measured at the outlet of plot P are quite sim-
13 ilar for the two rainfall events. The graph also shows that the soil fragments from plot P
14 settle faster than the soil fragments that leave plot P+TB. In fact, for the settling velocity
15 distribution measured for the sediments from plot P+TB, more than 40 % of the particles
16 were slower than $4.2 \cdot 10^{-4} \text{ m} \cdot \text{s}^{-1}$, whereas this velocity fraction represents only around
17 5 % of the sediments leaving plot P. This result suggests that the sediments entering the
18 tree belt are significantly denser than those leaving the tree belt.

19 **Nature of the sediments**

20 Complementary information on the nature of the fractions were obtained by visual ob-
21 servation of the collected sediments. The runoff at the outlet of plot P was a turbid,
22 light brown suspension without visible coarse particles. The colour of the suspension
23 suggests the sediments were predominately Mineral Soil Fragments (MSF). For the pre-
24 wetting rainfall event, the sediments leaving plot P contained some plant debris which
25 was washed from the bare soil zone. At the outlet of plot TB, the runoff was a relatively
26 clear suspension containing organic debris. Thus, the sediments leaving the tree belt con-

1 sisted of Coarse Organic Fragments (COF). A close look at the COF shows mostly leaves
2 (whole or fragmented) of *Calistemon* spp. and *Acacia* spp., small sticks, and grass frag-
3 ments. The runoff from plot P+TB was a light turbid suspension of organic debris with
4 the same composition as that for plot TB. Thus, the sediments from plot P+TB were a mix
5 of MSF and COF. The oversize runoff samples from plots TB and P+TB, contained only
6 COF. So, the total net masses of the oversize sediment fractions from these plots equal to
7 the masses of oversize COF.

8 The wet and dry bulk densities of the oversize COF are given in Table 3. These bulk
9 densities of less than $1 \text{ g}\cdot\text{cm}^{-3}$, are low compared to the soil aggregate bulk density (e.g.
10 see [Chepil, 1950](#); [Park and Smucker, 2005](#)) and water density. So, the COF is a light solid
11 fraction that floats in water.

12 These observations are consistent with the ASD (Figure 5) as well as the settling
13 velocity distribution (Figure 6) data. The sediments from plot TB have a coarse size
14 distribution without fractions finer than $10 \mu\text{m}$. The sediments from plot P have a finer size
15 distribution, with a small proportion of coarse size fractions, but a high settling velocity.
16 And the sediments from plot P+TB have a coarse size distribution, quite similar to the
17 ASD of plot TB with a higher proportion of fine fractions, but show a smaller settling
18 velocity.

19 **Total sediment budget**

20 The total mass of sediment at the outlet of the different plots, as well as the sediment
21 budget for the two events, are given in Table 4. The pasture area shows the highest ero-
22 sion rates with 0.95 and $1.98 \text{ t}\cdot\text{ha}^{-1}$ for event # 1 and event # 2, respectively. The erosion
23 rate is far lower for the tree belt zone with values at 0.002 and $0.039 \text{ t}\cdot\text{ha}^{-1}$ for event # 1
24 and event # 2, respectively. The whole system, pasture + tree belt, has an intermediate
25 erosion rate with 0.031 and $0.089 \text{ t}\cdot\text{ha}^{-1}$ for event # 1 and event # 2, respectively. For
26 ungrullied grazing landscapes in an adjacent catchment, [Armstrong and Mackenzie \(2002\)](#)
27 found average specific sediment yield of the same order ($0.07 \text{ t}\cdot\text{ha}^{-1}\cdot\text{y}^{-1}$). The high STR

1 values, largely above 0.90, show that the tested tree belt was very efficient in trapping
2 the sediment, even for intense rainfall conditions simulated in this experiment. The trap-
3 ping efficiency was not significantly influenced by the rainfall intensity: the STR value
4 decreased only very slightly between event # 1 and event # 2, while there was a 35 %
5 increase in the rainfall intensity.

6 **Sediment budgets by constituents**

7 The measurements showed that the sediment composition consisted of at least two con-
8 stituents: Mineral Soil Fragments (MSF) and Coarse Organic Fragments (COF).

9 COF were not observed in the particulate matter entering the tree belt (samples from
10 plot P). No COF were delivered to the tree belt and, subsequently, trapped within. COF
11 were present in samples collected at the outlet of the tree belt (samples from plot TB and
12 P+TB). So there is a net production of COF within the tree belt and this mass can this
13 directly be determined by the measurements at the outlet of plot P+TB.

14 The relative volume proportion of COF and MSF of the undersize sediments from plot
15 P+TB was determined by comparing the average ASD from plot TB and that from plot
16 P+TB. The assumptions underlying this comparison are:

- 17 1. the sediments collected at the outlet of plot P+TB are a mix of two constituents,
18 COF and MSF;
- 19 2. the sediments collected at the outlet of plot TB contain only COF;
- 20 3. the average ASD measured on the samples from plot TB, specifically the high pro-
21 portion of 479-to-1660 μm size fraction, is specific to the COF;
- 22 4. the COF from plot P+TB have the same ASD as the COF sampled from plot TB;
- 23 5. the 479-to-1660 μm size fraction of the sediments from plot P+TB only consisted
24 of COF. This last assumption is supported by the fact that the coarse fraction that
25 remained after sieving contained only COF.

1 The comparison was performed with the frequency distribution in order to avoid compli-
2 cation inherent in comparing cumulative distributions. To evaluate the fit, the Root Mean
3 Square Error (RMSE) was computed for the size fraction characteristic of the COF, i.e.
4 the 479-to-1660 μm size fraction, as well as the two adjacent size fractions, of 417-to-
5 479 μm and 1660-to-1905 μm . As the ASD for the sediments yield from plot TB during
6 event # 1 was not measured, the comparison was only performed for the data of event # 2.
7 The minimum RMSE was obtained for a volume proportion of COF set at 90.1 %. The
8 resulting fit is shown in Figure 7.

9 Knowing the volume proportion as well as the total mass of the undersize fraction and
10 the dry bulk densities of COF and MSF, we can then compute the total mass of undersize
11 COF and MSF. The dry bulk density of COF was measured and is given in Table 3. Soil
12 fragments have a wide range of bulk density (see [Chepil, 1950](#); [Park and Smucker, 2005](#)),
13 from less than $1.4 \text{ g}\cdot\text{cm}^{-3}$ for large aggregates to around $2.6 \text{ g}\cdot\text{cm}^{-3}$ for quartz particles,
14 so we used a range of values for the MSF bulk density. The mass of the undersize fraction
15 was determined by weighing. About 1.5 to 1.8 kg of undersize COF was produced by
16 the tree belt of plot P+TB, during event # 2. By adding the mass of the oversize fraction,
17 which contained only COF, the total mass of COF produced by the tree belt is in the
18 range of 1.8 to 2.1 kg. The total mass of MSF from plot P+TB is between 0.6 to 0.9 kg.
19 Considering that the sediments delivered to the tree belt were only made of MSF and
20 that no MSF were produced within the tree belt, the MSF trapping ratio for event # 2 is
21 between 98 and 99 %.

22 **Sediment budgets by size fractions**

23 The ASD of the MSF from plot P+TB for event # 2 is computed from the difference
24 between the COF size distribution fitted in the previous section (see Figure 7), and the
25 ASD of the total sediments leaving this plot during the same event (see Figure 5). The
26 computed MSF size distribution ranges from $1.1 \mu\text{m}$ to $209 \mu\text{m}$ (see Figure 8).

27 Knowing the ASDs as well as the total mass of MSF entering and leaving the tree belt,

1 trapping ratios by size fraction can then be computed from Equation 5. For this computa-
2 tion, we used an average bulk density of $2.2 \text{ g}\cdot\text{cm}^{-3}$ which was determined from the values
3 measured by [Chepil \(1950\)](#) for silt loam aggregates in the size fractions $< 100 \text{ }\mu\text{m}$ and
4 $100\text{--}500 \text{ }\mu\text{m}$. As shown on Figure 9, the STRs are very high for all the size fractions with
5 a minimum of 91 % and a maximum of 100 %. For the finest (from 0.32 to $1.3 \text{ }\mu\text{m}$) and
6 the coarsest (above $182 \text{ }\mu\text{m}$) MSF, the whole mass from plot P was trapped within the tree
7 belt and no fragments from these size fractions were detected at the outlet of plot P+TB
8 (see Figure 8). For the medium size fractions, the STR is dependent on the fragment size.
9 From 1.3 to $9 \text{ }\mu\text{m}$ the STR decreases regularly when the fragment size increases and it
10 reaches a minimum between 9 and $15 \text{ }\mu\text{m}$. From $15 \text{ }\mu\text{m}$ to $182 \text{ }\mu\text{m}$, the STR increases
11 with the size.

12 Discussion

13 Total trapping efficiency

14 Even for intense rainfall events (ARI around 10 and 50 y), the sediment trapping in the tree
15 belt was very efficient, with a global and minimum STR of 95 and 94 % for events # 1
16 and 2, respectively. Even for the most intense rainstorm, event # 2, the MSF trapping
17 ratio was 98–99 %. These high values show that the tree belt is able to trap most of
18 the sediments even for extreme conditions such as exceptional rainstorm or concentrated
19 flow. These STRs lie at the upper end of the reported range and are consistent with
20 most of the values given in the literature for VFSs (e.g. see the reviews by [Dosskey,](#)
21 [2001](#); [Helmerts et al., 2005](#)). For example, [Helmerts et al. \(2005\)](#) report STR values from
22 41 to 100 % with a median of 88 %. However, most of the published studies concern
23 grass buffers alone or combined with a wooded strip located downslope. The trapping
24 efficiency of forested area alone has been rarely investigated. From the data reported in
25 Table 2 of [Lee et al. \(2000\)](#), STRs for a 9.2 m long woody (shrubs and tree) buffer can
26 be computed. In their experiment, 65 to 73 % of the sediments were trapped within the

1 woody buffer. The sediment loads measured by [Sheridan et al. \(1999\)](#) (see their Table 7)
2 at approximately 5 m (position 2) and 30 m (position 3) from the entrance of a forest
3 riparian buffer show that, at least, 22 to 60 % of the sediment mass was trapped in this
4 wooded area. Comparing inflow and outflow sediment concentrations for 12 short (0.5
5 to 3-m-long) forest plots, [Loch et al. \(1999\)](#) determined transport efficiencies from 16
6 to 98 %, which correspond to trapping efficiencies ranging from 2 to 84 %. Using the
7 same computation procedure, [Hairsine \(1996\)](#) determined a trapping efficiency greater
8 than 90 % for a 6-m-long near-natural riparian forest. Using ¹³⁷Cs, [Cooper et al. \(1987\)](#)
9 showed that, for a North Carolina watershed, 42 to 45 % of the sediments removed from
10 the cultivated fields over 20 y, were deposited within the first 100 m of a riparian forest.
11 These results suggest that the sediment trapping efficiency should be more variable for
12 forested than for grass filter strips and that very high trapping efficiencies can be expected
13 for forested buffers.

14 The high variability of sediment trapping for forested areas is probably related to
15 the wide range of observed soil surface conditions: potential development of herbaceous
16 cover; possible presence of tree residues; variation in the extension, the thickness and
17 the nature of surface litter (e.g. see the site descriptions given by [Loch et al., 1999](#)).
18 Moreover, the flow characteristics seem to be more heterogeneous in forested than in
19 grass areas ([Mackenzie and Hairsine, 1996](#)). As suggested by [Darboux et al. \(2001\)](#), a
20 small local change in roughness at the centimetre scale can have a major impact on runoff
21 and, consequently, on sediment delivery at the plot scale.

22 For our experiment, the rates of runoff capture by the tree belt were largely lower (32
23 to 68 % in event # 1, and 0 to 28 % in event # 2) than the sediment trapping ratios. In
24 the experimental data reviewed by [Dosskey \(2001\)](#), the water flow reductions are always
25 lower than the corresponding sediment trapping ratios. The same pattern was observed
26 by [Daniels and Gilliam \(1996\)](#) and [Le Bissonnais et al. \(2004\)](#) among others. All these
27 experimental results point out that sediment trapping processes are only partly linked to
28 the water capture processes.

1 **Trapping efficiency by size fractions**

2 The STRs, computed by MSF size fraction, indicate that, at least for event # 2, there
3 was a selective trapping of the coarsest ($> 182 \mu\text{m}$) and finest ($< 1.3 \mu\text{m}$) fragments.
4 The selective trapping of the coarsest soil fragments, often $> 125 \mu\text{m}$, is well known for
5 all kind of VFSs (Dabney et al., 1995; Meyer et al., 1995; Loch et al., 1999; Lee et al.,
6 2000; Ghadiri et al., 2001; Jin and Römken, 2001; Jin et al., 2002; Le Bissonnais et al.,
7 2004; Deletic, 2005, 2006). The trapping of the coarse size fractions is due to the greater
8 settling velocities of these fragments which tend to be very quickly deposited when the
9 flow slows (Dabney et al., 1995; Ghadiri et al., 2001; Deletic, 2001). Moreover, larger
10 fragments are also more easily trapped by obstruction in the litter. Consequently, the
11 ASD of the outflow is relatively enriched in fine fractions when compared to the inflow.
12 However reported mass budgets show also that the finest fragments can be trapped within
13 buffers: Jin et al. (2002) obtain STRs from 0 to 55 % for fragments $< 63 \mu\text{m}$; the data
14 from the Table 2 of Lee et al. (2000) show STRs for the clay fraction ranging from 27 to
15 71 %; in the flume experiments of Meyer et al. (1995), 20 % of the sediment fragments
16 from the size fractions under $32 \mu\text{m}$ were trapped. So, even if a large amount of fine soil
17 fragments can be trapped within a VFS, the selective retention of these fractions has not
18 been observed before. Nevertheless, the results presented in Table 2 of Lee et al. (2000)
19 show that the clay fraction is more efficiently trapped by the woody buffer than by the
20 grass buffer. The STRs for clay are 39 % higher for the woody area in comparison with
21 the grass strip whereas, for the sand and the silt fractions, the maximum differences are
22 only 18 and 9 % respectively. Our results, as well as those of Lee et al. (2000), suggest
23 that the trapping of the finest soil fragments could be more efficient in forested filter strips
24 than in the grass strips.

1 **Trapping processes**

2 The most obvious trapping process noticed during our experiment is sedimentation, i.e.
3 the process of deposition of sediment by water on the soil surface. Sedimentation first oc-
4 curred at the upslope of the tree belt due to backwater ponding. Backwater sedimentation
5 has been widely reported as a key trapping process from various field as well as laboratory
6 experiments (see e.g. [Dillaha et al., 1988](#); [Dabney et al., 1995](#); [Meyer et al., 1995](#); [Ghadiri](#)
7 [et al., 2001](#); [Lacas et al., 2005](#)) and it has been implemented in VFS models ([Hayes et al.,](#)
8 [1984](#); [Muñoz-Carpena et al., 1999](#); [Rose et al., 2002](#)). This process doesn't seem to be
9 as typical in wooded filter strips: it was observed only for 1 out of the 12 experimental
10 plots tested by [Loch et al. \(1999\)](#). However their experimental conditions were purposely
11 set to avoid sedimentation in the feeding area of the buffer, and, consequently, were not
12 conducive to backwater trapping. In our experiment, backwater sedimentation seems to
13 be the dominant form of sediment trapping. In fact, for the two rainfall events, a total
14 sediment mass of about 38 kg settled in the backwater (see page 13), which corresponds
15 to 66 % and 62 % of the total sediment masses respectively trapped by the tree belt and
16 leaving the pasture (see Table 4). Sedimentation also occurred within the tree belt itself,
17 upslope of the small litter dams that formed during the rainfall events. This deposition
18 led to the formation of micro-terraces. In comparison with the backwater deposit, the
19 micro-terraces were thinner (no more than 1 mm) and extended over a small area (very
20 patchy and mainly in the first 1.5 m of the concentrated flow paths). Consequently, the
21 mass of sediment trapped in these features is not as important as in the backwater.

22 In the two deposition areas described above, the sedimentation is due to a retardance
23 of the overland flow caused by the accumulation, on the soil surface of the tree belt area, of
24 litter debris organised as a continuous cover or as barriers. The increased flow retardance
25 within the tree belt is evidenced by the higher values of Manning's hydraulic roughness
26 coefficient for this area compared with the pasture plot (see Table 2). The control of bed
27 hydraulic roughness on the backwater flow characteristics is clearly showed by [Ghadiri](#)
28 [et al. \(2001\)](#) and [Rose et al. \(2002\)](#). Thus, the litter cover was a key surface condition

1 feature for modifying the water flow and trapping sediments. Such an important role of the
2 tree litter has already been concluded by [Daniels and Gilliam \(1996\)](#) and [Hairsine \(1996\)](#).
3 However, with the action of the overland flow, the litter was drastically reorganised and a
4 significant proportion was exported out of the tree belt as attested by the important mass
5 of COF measured at the tree belt outlet during event # 2 (1.8 to 2.1 kg of exported COF).
6 This erosion did not lead to the disappearance of the litter cover and the trapping features
7 were not disrupted even if the simulated rainfall events were extreme. This observation
8 indicates that the trapping capacity of the tree belt should remain on a time scale longer
9 than a rainfall event. However to assess the long-term trapping efficiency, the dynamics
10 of the litter cover should be studied.

11 The simple settling theory has been successfully used to reproduce the size selectiv-
12 ity over an area of deposition ([Dabney et al., 1995](#); [Beuselinck et al., 1999a](#)). To assess
13 the size selectivity of this process for our experimental conditions, we used the backwa-
14 ter sedimentation model, based on the simple settling theory, proposed by [Dabney et al.](#)
15 ([1995](#)). The settling velocities were computed from the size distributions, using the algo-
16 rithm of [Cheng \(1997\)](#) with a bulk density of $2.2 \text{ g}\cdot\text{cm}^{-3}$ for wet soil aggregates ([Rhoton](#)
17 [et al., 1983](#)). The backwater length was assumed to be equal to the length of the deposit,
18 i.e. 60 cm. The model predicts that the fragments coarser than 50 and 75 μm , for respec-
19 tively events # 1 and # 2, should be all trapped within the backwater. No fragments finer
20 than 3 μm should settle in the backwater. Thus, this process could be responsible for the
21 high trapping ratio for the coarsest MSF (see [Figure 9](#)) but cannot explain the trapping of
22 the fine fractions observed during our experiments.

23 Another trapping process noticed during the experiment is the macropore infilling.
24 The penetration of particles, originated from the soil surface, in the soil profile has al-
25 ready been suggested by [Øygarden et al. \(1997\)](#) and [Hardy et al. \(1999\)](#). The effects of
26 biological macropores on runoff and infiltration have been studied in details by [Léonard](#)
27 [et al. \(2004\)](#) but, to our knowledge, the consequences on sediment transport have not
28 been examined yet. In consequence, no information are available about an eventual size

1 selectivity of this trapping process. However, as the macropores were filled at the end of
2 event # 1, this process cannot be invoked for the high trapping of fine fractions measured
3 during event # 2. The clogging of the macropores caused a decline of the trapping capac-
4 ity of the tree belt. The recovery of this capacity should be linked to the reestablishment
5 of the macropores by biological activity. Thus the time to recovery should depend on the
6 status of the soil macrofauna. On our experimental site, macropores might return within
7 a week, as we noticed ants activity soon after the rain stopped.

8 [Dosskey \(2001\)](#) suggests that, similarly to dissolved compounds, colloids and clays
9 could be trapped by adsorption on soil surfaces, vegetation and organic debris. Such
10 a process could explain the selective trapping of the fine fractions observed in our ex-
11 periment. The capture by adsorption of colloids transported in a water flow has been
12 extensively studied within the soil profile (e.g. see [DeNovio et al., 2004](#); [Kanti Sen and](#)
13 [Khilar, 2006](#)) but, to our knowledge, has not been described at the soil surface. However
14 the importance of adsorption of molecules in solution has been widely shown in VFS and
15 its control parameters have been identified (e.g. see the reviews of [Dosskey, 2001](#); [Lacas](#)
16 [et al., 2005](#)). During our experiment, the water was forced to flow through the litter cover
17 and barriers present at the surface of the tree area. As the above ground plant debris have
18 a high adsorption capacity ([Benoit et al., 1999](#); [Lickfeldt and Branham, 1995](#)), it is likely
19 that the finest soil fragments transported in the overland flow were captured by adsorption
20 on the litter. Such a process could act on the fraction not trapped by the sedimentation
21 process, i.e. the $< 3 \mu\text{m}$ fraction. For event # 2, this means that, about 960 g of sediments
22 (i.e. the total mass of soil fragments under $3 \mu\text{m}$ trapped within the tree belt) should be
23 trapped on the surface of the litter debris. This represents only 3 % and 2 % of the total
24 sediment masses respectively trapped by the tree belt and exported from the pasture (see
25 [Table 4](#)).

1 Conclusion

2 In this paper, we examined the sediment trapping capacity of a tree belt used as a VFS by
3 analysing data and observations gathered during field rainfall simulations. The computed
4 sediment budgets show that, even for intense rainfall conditions similar to concentrated
5 flow conditions, the studied tree belt was able to trap a high proportion of the delivered
6 sediments: STR was around 95 %. These values are slightly higher than the few STRs
7 reported in the literature for forested buffers. The STRs by size fraction computed for the
8 most intense rainfall event lie between 91 and 100 % with a minimum for the medium-
9 sized fragments. Selective trapping of coarse size fraction is widely reported for VFS and
10 is linked to the sedimentation process. In these circumstances, selective trapping of the
11 soil fragments under 3 μm has never been recorded before to our knowledge.

12 The sediment budgets combined with observations of the soil surface conditions en-
13 able us to identify different processes which trap sediment within a tree belt. The main
14 trapping process is the sedimentation in the backwater zone (62 % of the trapped sedi-
15 ments) and at the micro-terraces formed in the tree belt area. This process is related to
16 the thick litter cover present within the tree belt. The sedimentation trapped the major-
17 ity of the total sediment mass and selectively the coarsest size fractions. These results
18 are consistent with other literature data. We also clearly identified the trapping effect of
19 the macropores, a process which was only suspected before ([Dosskey, 2001](#); [Lacas et al.,](#)
20 [2005](#)). Although not confirmed, it is likely that the finest soil fragments transported in
21 overland flow were trapped by adsorption on the numerous litter debris located in the tree
22 belt area. Even if such a process could trap only a very small quantity of sediment, it is
23 crucial to consider it as it concerns the finest fragments which have the highest polluting
24 capacity. This experiment enabled us to identify and to quantify relatively the trapping
25 processes and their effects in term of sediment size distribution for a tree belt. The trap-
26 ping processes identified here are not specific to tree belts and may be present in other
27 types of VFSs.

28 The main soil surface features that favoured trapping were the litter cover and the

1 macropore openings. During the rainfall events, these features were greatly affected by
2 the overland flow. In consequence, the monitoring of the evolution through time of litter
3 cover and biological macropores is necessary to assess the long-term trapping efficiency
4 of the tree belt.

5 **Acknowledgements**

6 The authors are grateful to David Marsh, who encouraged this experiment to be con-
7 ducted on his land; Jim Brophy, who managed the experimental setup and the rainfall
8 simulation; Peter Fogarty, who shared his experience on experimental design and helped
9 for the sampling; Jacky Croke, who gave advices on the experimental design; Martyn El-
10 lis who helped for the experimental setup; all the colleagues from the CSIRO Integrated
11 Catchment Management team who assisted in the sampling and the data recording; and
12 Brian G. Jones, associate professor at Wollongong University, to allow us access to the
13 laser diffraction sizer.

1 **References**

- 2 Armstrong, J. L. and Mackenzie, D. H. (2002). Sediment yields and turbidity records
3 from small upland subcatchments in the Warragamba Dam Catchment, southern New
4 South Wales. *Australian Journal of Soil Research*, 40(4):557–579.
- 5 Auzet, A.-V., Boiffin, J., Papy, F., Ludwig, B., and Maucorps, J. (1993). Rill erosion as a
6 function of the characteristics of cultivated catchments in the North of France. *Catena*,
7 20:41–62.
- 8 Baudry, J., Bunce, R. G. H., and Burel, F. (2000). Hedgerows: An international perspec-
9 tive on their origin, function and management. *Journal of Environmental Management*,
10 60(1):7–22.
- 11 Benoit, P., Barriuso, E., Vidon, P., and Réal, B. (1999). Isoproturon sorption and degra-
12 dation in a soil from grassed buffer strip. *Journal of Environmental Quality*, 28:1–9.
- 13 Beuselinck, L., Govers, G., Steegen, A., Hairsine, P. B., and Poesen, J. (1999a). Evalua-
14 tion of the simple settling theory for predicting sediment deposition by overland flow.
15 *Earth Surface Processes and Landforms*, 24:993–1007.
- 16 Beuselinck, L., Govers, G., Steegen, A., and Quine, T. A. (1999b). Sediment transport
17 by overland flow over an area of net deposition. *Hydrological Processes*, 13(17):2769–
18 2782.
- 19 Bos, M. G., Replogle, J. A., and Clemmens, A. J. (1991). *Flow measuring flumes for open*
20 *channel systems*. American Society of Agricultural Engineers, St Joseph, Michigan,
21 USA.
- 22 Canterford, R. P., Pescod, N. R., J, P. H., and Turner, L. H. (1987). *Design intensity-*
23 *frequency-duration rainfall*, chapter 2, pages 13–40. The Institution of Engineers,
24 Australia, 3rd edition.

- 1 Cheng, N.-S. (1997). Simplified settling velocity formula for sediment particle. *Journal*
2 *of Hydraulic Engineering*, February:149–152.
- 3 Chepil, W. S. (1950). Methods of estimating apparent density of discrete soil grains and
4 aggregates. *Soil Science*, 70:351–362.
- 5 Cooper, J. R., Gilliam, J. W., Daniels, R. B., and Robarge, W. P. (1987). Riparian areas as
6 filters for agricultural sediment. *Soil Science Society of America Journal*, 51(2):416–
7 420.
- 8 Dabney, S. M., Meyer, L. D., Harmon, W. C., Alonso, C. V., and Foster, G. R. (1995). De-
9 positional patterns of sediment trapped by grass hedges. *Transactions of the American*
10 *Society of Agricultural Engineers*, 38(6):1719–1729.
- 11 Daniels, R. B. and Gilliam, J. W. (1996). Sediment and chemical load reduction by grass
12 and riparian filters. *Soil Science Society of America Journal*, 60(1):246–251.
- 13 Darboux, F., Davy, P., Gascuel-Oudou, C., and Huang, C. (2001). Evolution of soil surface
14 roughness and flowpath connectivity in overland flow experiments. *Catena*, 46:125–139.
- 15 Deletic, A. (2001). Modelling of water and sediment transport over grassed areas. *Journal*
16 *of Hydrology*, 248:168–182.
- 17 Deletic, A. (2005). Sediment transport in urban runoff over grassed areas. *Journal of*
18 *Hydrology*, 301:108–122.
- 19 Deletic, A. (2006). Performance of grass filters used for stormwater treatment — a field
20 and modelling study. *Journal of Hydrology*, 317:261–275.
- 21 DeNovio, N. M., Saiers, J. E., and Ryan, J. N. (2004). Colloid movement in unsaturated
22 porous media: recent advances and future directions. *Vadose Zone Journal*, 3:338–351.
- 23 Dillaha, T. A., Reneau, R. B., Mostaghimi, S., and Lee, D. (1989). Vegetative filter strips
24 for agricultural nonpoint source pollution control. *Transactions of the American Society*
25 *of Agricultural Engineers*, 32(2):513–519.

- 1 Dillaha, T. A., Sherrard, J. H., Lee, D., S, M., and Shanholtz, V. O. (1988). Evaluation
2 of vegetative filter strips as a best management practice for feed lots. *Journal of Water*
3 *Pollution Control Federation*, 60:1231–1238.
- 4 Dosskey, M. J. (2001). Toward quantifying water pollution abatement in response to
5 installing buffers on crop land. *Environmental Management*, 28(5):577–598.
- 6 Dosskey, M. J. (2002). Setting priorities for research on pollution reduction functions of
7 agricultural buffers. *Environmental Management*, 30(5):641–650.
- 8 Driessen, P., Deckers, J., Spaargaren, O., and Nachtergaele, F., editors (2001). *Lecture*
9 *notes on the major soils of the world*, number 94 in Soil Resources Reports, Roma.
10 Food and Agriculture Organization of the United Nations.
- 11 Droppelmann, K. and Berliner, P. (2003). Runoff agroforestry — a technique to secure the
12 livelihood of pastoralists in the middle east. *Journal of Arid Environments*, 54(3):571–
13 577.
- 14 Ellis, T. W., Leguédou, S., Hairsine, P. B., and Tongway, D. J. (2006). Capture of overland
15 flow by a tree belt on a pastured hillslope in south-eastern Australia. *Australian Journal*
16 *of Soil Research*, 44:117–125.
- 17 Ghadiri, H., Rose, C. W., and Hogarth, W. L. (2001). The influence of grass and porous
18 barrier strips on runoff hydrology and sediment transport. *Transactions of the American*
19 *Society of Agricultural Engineers*, 44:259–268.
- 20 Hairsine, P. B. (1996). Comparing grass filter strips and near-natural riparian forests for
21 buffering intense hillslope sediment sources. In Rutherford, I. and Walker, M., editors,
22 *Proceedings of First National Conference on Stream Management in Australia*, pages
23 203–206. Cooperative Research Centre for Catchment Hydrology, Merrijiig, Australia.
- 24 Hairsine, P. B. and McTainsh, G. (1986). The Griffith tube: A simple settling tube for

- 1 the measurement of settling velocity of aggregates. Technical Report 3/86, School of
2 Australian Environmental Studies, Griffith University, Australia.
- 3 Hardy, I. A. J., Garter, A. D., Leeds-Harrison, P. B., Sanders, R. M., and I, F. (1999). The
4 origin of sediments in field drainage water. In *Tracers in Geomorphology*. John Wiley
5 and Sons.
- 6 Hayes, J. C., Barfield, B. L., and Barnhisel, R. I. (1984). Performance of grass filters under
7 laboratory and field conditions. *Transactions of the American Society of Agricultural*
8 *Engineers*, 27:1321–1331.
- 9 Helmers, M. J., Eisenhauer, D. E., Dosskey, M. G., Franti, T. G., Brothers, J. M., and Mc-
10 Cullough, M. C. (2005). Flow pathways and sediment trapping in a field-scale vegeta-
11 tive filter. *Transactions of the American Society of Agricultural Engineers*, 48(3):955–
12 968.
- 13 Jin, C.-X., Dabney, S. M., and Römken, M. J. M. (2002). Trapped mulch increases
14 sediment removal by vegetative filter strips: a flume study. *Transactions of the American*
15 *Society of Agricultural Engineers*, 45(4):929–939.
- 16 Jin, C.-X. and Römken, M. J. M. (2001). Experimental studies of factors in determining
17 sediment trapping in vegetative filter strips. *Transactions of the American Society of*
18 *Agricultural Engineers*, 44(2):277–288.
- 19 Kang, B. T., L, R., and Atta-Krah, A. N. (1990). Alley farming. *Advances in Agronomy*,
20 43:315–359.
- 21 Kanti Sen, T. and Khilar, K. C. (2006). Review on subsurface colloids and colloid-
22 associated contaminant transport in saturated porous media. *Advances in Colloid and*
23 *Interface Science*, 119(2–3):71–96.
- 24 Lacas, J.-G., Voltz, M., Gouy, V., Carlier, N., and Gril, J.-J. (2005). Using grassed

- 1 strips to limit pesticide transfer to surface water: a review. *Agronomical Sustainable*
2 *Development*, 25(2):253–266.
- 3 Le Bissonnais, Y., Lecomte, V., and Cerdan, O. (2004). Grass strip effects on runoff and
4 soil loss. *Agronomie*, 24:129–136.
- 5 Lee, D., Dillaha, T. A., and Sherrard, J. H. (1989). Modeling phosphorus transport in
6 grass buffer strips. *Journal of Environmental Engineering*, 115(2):409–427.
- 7 Lee, K.-H., Isenhardt, T. M., Schultz, R. C., and Mickelson, S. K. (2000). Multispecies
8 riparian buffers trap sediment and nutrients during rainfall simulations. *Journal of*
9 *Environmental Quality*, 29:1200–1205.
- 10 Léonard, J., Perrier, E., and Rajot, J.-L. (2004). Biological macropores effect on runoff
11 and infiltration: a combined experimental and modelling approach. *Agriculture,*
12 *Ecosystems and Environment*, 104:277–285.
- 13 Lickfeldt, D. W. and Branham, B. E. (1995). Sorption of nonionic compounds by ken-
14 tucky bluegrass leaves and thatch. *Journal of Environmental Quality*, 24:980–985.
- 15 Loch, R. J. (2001). Settling velocity — a new approach to assessing soil and sediment
16 properties. *Computers and Electronics in Agriculture*, 31:305–316.
- 17 Loch, R. J., Espigares, T., Costantini, A., Garthe, R., and Bubb, K. (1999). Vegetative
18 filter strips to control sediment movement in forest plantations: validation of a simple
19 model using field data. *Australian Journal of Soil Research*, 37(5):929–946.
- 20 Mackenzie, D. H. and Hairsine, P. B. (1996). The hydraulics of shallow overland flow:
21 a comparison between a grass filter strip and a near-natural riparian forest. In Ruther-
22 furd, I. and Walker, M., editors, *Proceedings of First National Conference on Stream*
23 *Management in Australia*, pages 207–211. Cooperative Research Centre for Catchment
24 Hydrology, Merrijig, Australia.

- 1 Meyer, L. D., Dabney, S. M., and Harmon, W. C. (1995). Sediment-trapping effectiveness
2 of stiff-grass hedges. *Transactions of the American Society of Agricultural Engineers*,
3 38(3):809–815.
- 4 Muñoz-Carpena, R. and Parsons, J. E. (2004). A design procedure for vegetative filter
5 strip using VFSSMOD-W. *Transactions of the American Society of Agricultural Engi-*
6 *neers*, 47(6):1933–1941.
- 7 Muñoz-Carpena, R., Parsons, J. E., and Gilliam, J. W. (1999). Modeling hydrology and
8 sediment transport in vegetative filter strips. *Journal of Hydrology*, 214(1/4):111–129.
- 9 Øygarden, L., Kvaerner, J., and Jenssen, P. D. (1997). Soil erosion via preferential flow
10 to drainage systems in clay soils. *Geoderma*, 76(1–2):65–86.
- 11 Park, E.-J. and Smucker, A. J. M. (2005). Erosive strengths of concentric regions within
12 soil macroaggregates. *Soil Science Society of America Journal*, 69(6):1912–1921.
- 13 Regent Instrument INC (2005). *WinRHIZO for root analysis*. Regent Instrument INC.
- 14 Rhoton, F. E., Meyer, L. D., and Whisler, F. D. (1983). Densities of wet aggregated sedi-
15 ment from different textured soils. *Soil Science Society of America Journal*, 47(3):576–
16 578.
- 17 Rose, C. W., Hogarth, W. L., Ghadiri, H., Parlange, J.-Y., and Okom, A. (2002). Overland
18 flow to and through a segment of uniform resistance. *Journal of Hydrology*, 255:134–
19 150.
- 20 Schmitt, T. J., Dosskey, M. G., and Hoagland, K. D. (1999). Filter strip performance and
21 process for different vegetation, widths, and contaminants. *Journal of Environmental*
22 *Quality*, 28:1479–1489.
- 23 Sheridan, J. M., Lowrance, R., and Bosch, D. D. (1999). Management effects on runoff
24 and sediment transport in riparian forest buffers. *Transactions of the American Society*
25 *of Agricultural Engineers*, 42(1):55–64.

- 1 Stirzaker, R., Vertessy, R., and Sarre, A., editors (2002). *Trees, water and salt. An Aus-*
2 *tralian guide to using trees for healthy catchments and productive farms*, Barton, Aus-
3 tralia. Joint Venture Agroforestry Program, CSIRO, Cooperative Research Centre for
4 Catchment Hydrology, Rural Industries Research and Development Corporation, Rural
5 Industries Research and Development Corporation.
- 6 Takken, I., Beuselinck, L., Nachtergaele, J., Govers, G., Poesen, J., and Degraer, G.
7 (1999). Spatial evaluation of a physically-based distributed erosion model LISEM.
8 *Catena*, 37:431–447.
- 9 Tongway, D. J. and Hindley, N. L. (2004). *Landscape function analysis manual: Proce-*
10 *dures for monitoring and assessing landscapes with special reference to minesites and*
11 *rangelands*. CSIRO Sustainable Ecosystems, Canberra, Australia.
- 12 van Dijk, P. M., Auzet, A.-V., and Lemmel, M. (2005). Rapid assessment of field erosion
13 and sediment transport pathways in cultivated catchments after heavy rainfall events.
14 *Earth Surface Processes and Landforms*, 30(2):169–182.
- 15 van Dijk, P. M., Kwaad, F. J. P. M., and Klapwijk, M. (1996). Retention of water and
16 sediment by grass strips. *Hydrological Processes*, 10:1069–1080.
- 17 Wilson, C. J. (1999). Effects of logging and fire on runoff and erosion on highly erodible
18 granitic soils in Tasmania. *Water Resources Research*, 35:3531–3546.

1 **List of Figures**

2	1	Plot layout of the experiment.	34
3	2	Comparison of the ASDs of samples sieved at 1680 and 595 μm	35
4	3	Litter dams and micro-terraces	36
5	4	Temporal evolution of the MWD of the ASDs	37
6	5	Average Fragment Size Distributions of the collected sediments.	38
7	6	Settling velocity distributions.	39
8	7	Fitting of the COF size distribution to the total sediment aggregate size distribution	40
9			
10	8	Computed ASDs of the COF and the MSF from plot P+TB, event # 2.	41
11	9	MSF budget by size fraction for rainfall event # 2	42

1 Figures

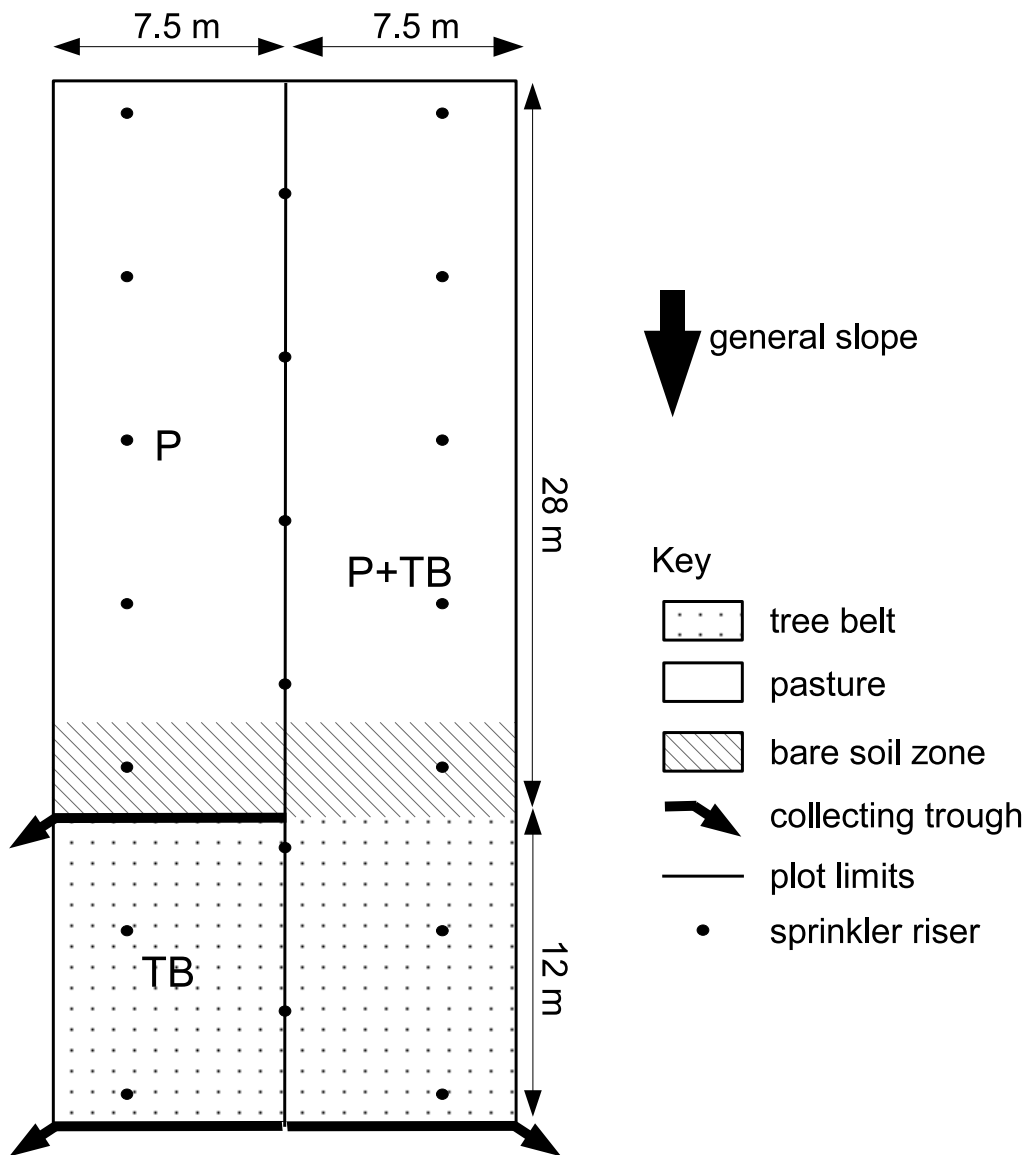


Figure 1: Plot layout (not drawn to scale) of the experiment.
P: pasture plot; TB: tree belt plot; P+TB: pasture + tree belt plot

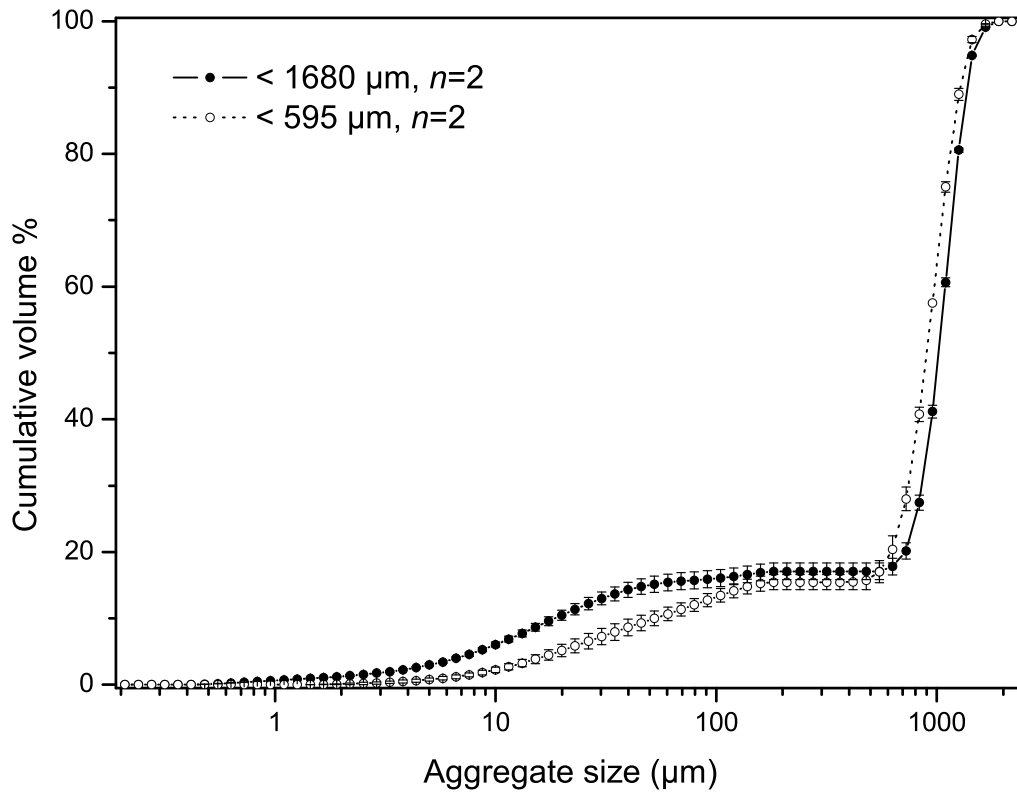


Figure 2: Comparison of the size distribution of samples obtained with sieve size 1680 and 595 μm from plot P+TB during event # 2. Error bars represent standard errors. n is the number of samples.

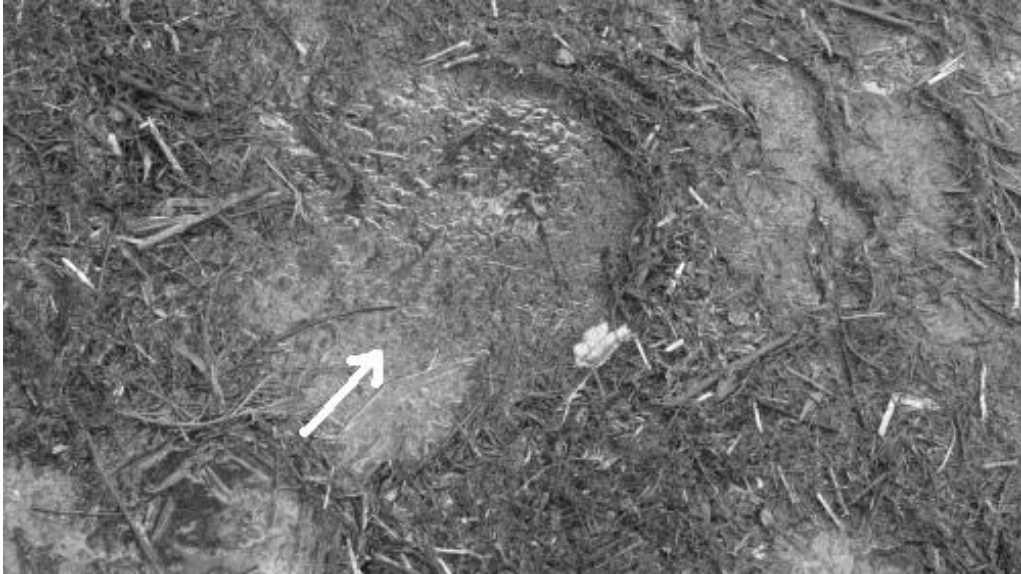


Figure 3: View of the litter dams and the related micro-terraces formed within the tree belt during the rainfall events.
The white arrow shows the flow direction.

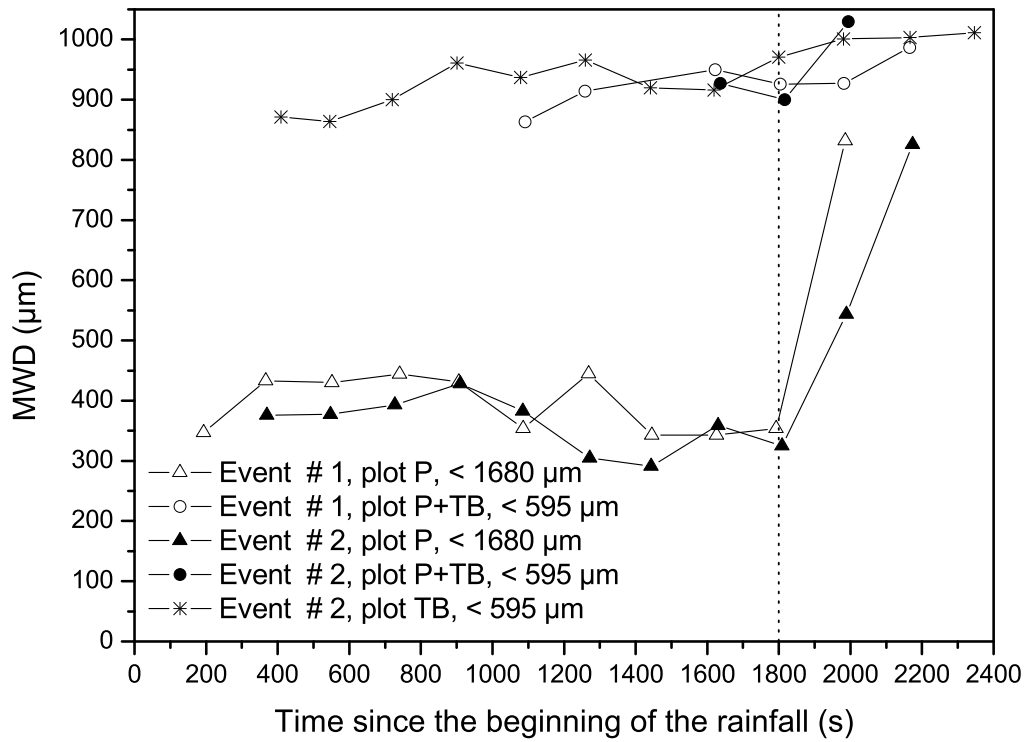


Figure 4: Temporal evolution of the Mean Weight Diameter of the Aggregate Size Distributions.

The vertical dashed line indicates the end of the rainfall simulation.

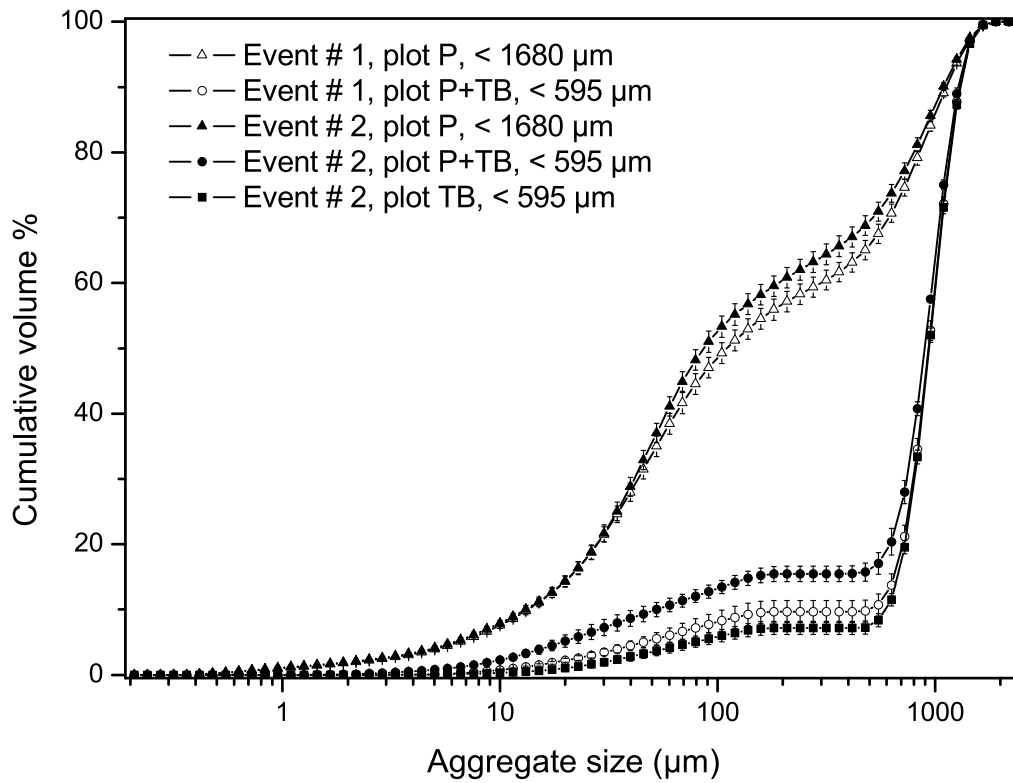


Figure 5: Average Aggregate Size Distributions (ASDs) of the sediments collected at the outlet of plots P, P+TB and TB during the rainfall period of events # 1 and # 2. The error bars represent the standard errors.

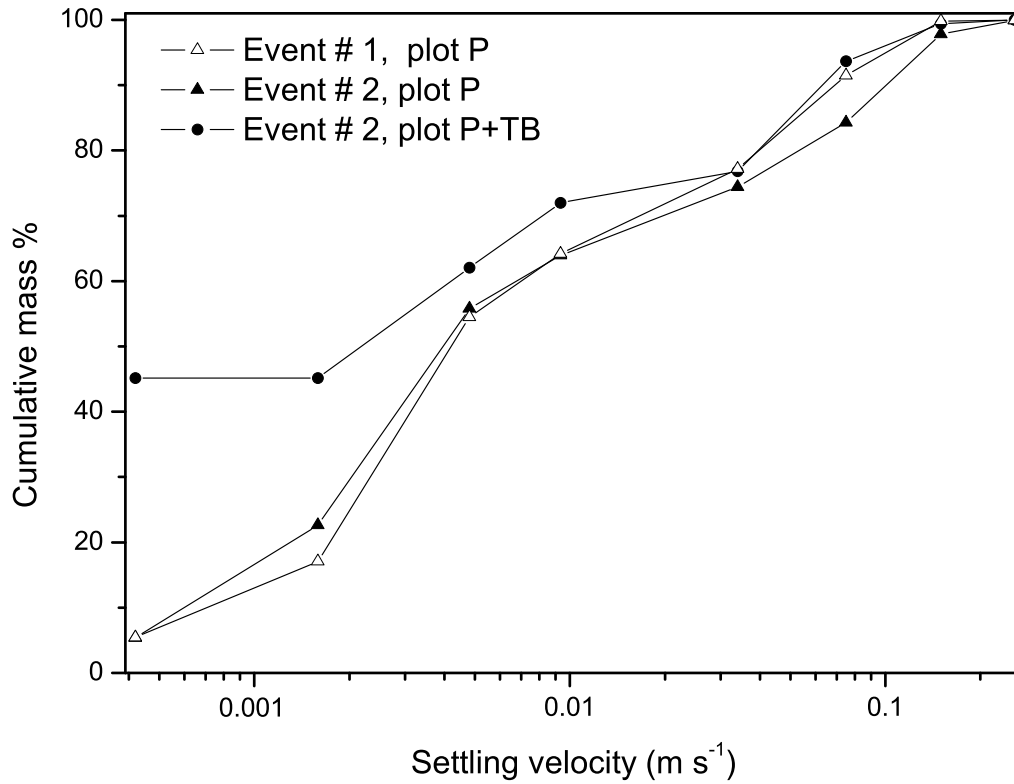


Figure 6: Settling velocity distributions measured for the sediment collected at the outlet of plot P during rainfall events # 1 and # 2, and plot P+TB during rainfall event # 2 respectively.

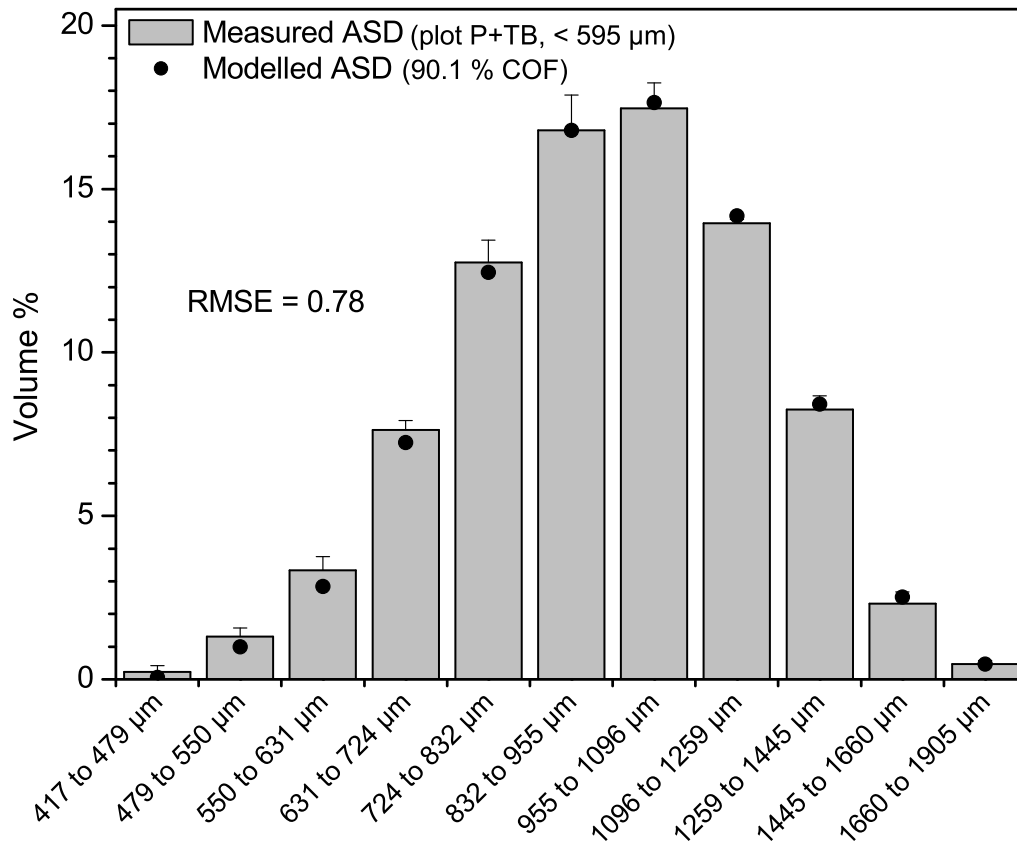


Figure 7: Fitting of the COF aggregate size distribution to the aggregate size distribution measured for plot P+TB for event # 2.

ASD: Aggregate Size Distribution; RMSE: Root Mean Square Error; COF: Coarse Organic Fragments.

The error bars represent the standard errors on the measured aggregate size distribution.

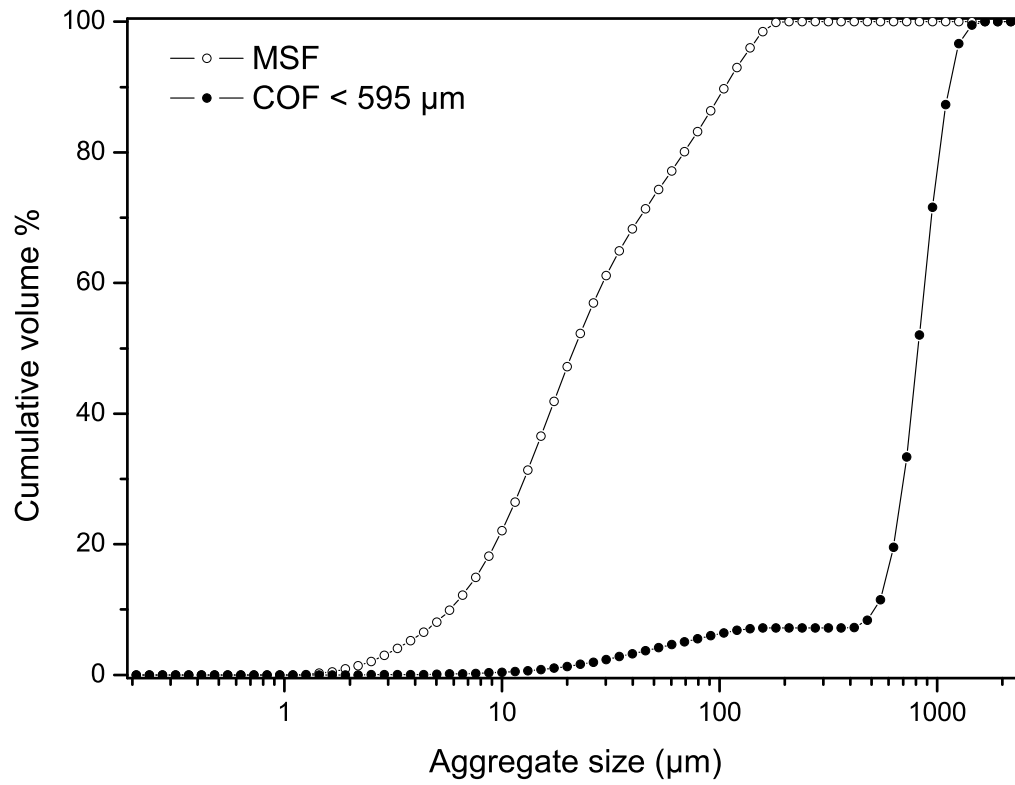


Figure 8: Aggregate size distributions of the COF and the MSF computed for plot P+TB, event # 2.

COF: Coarse Organic Fragments; MSF: Mineral Soil Fragments.

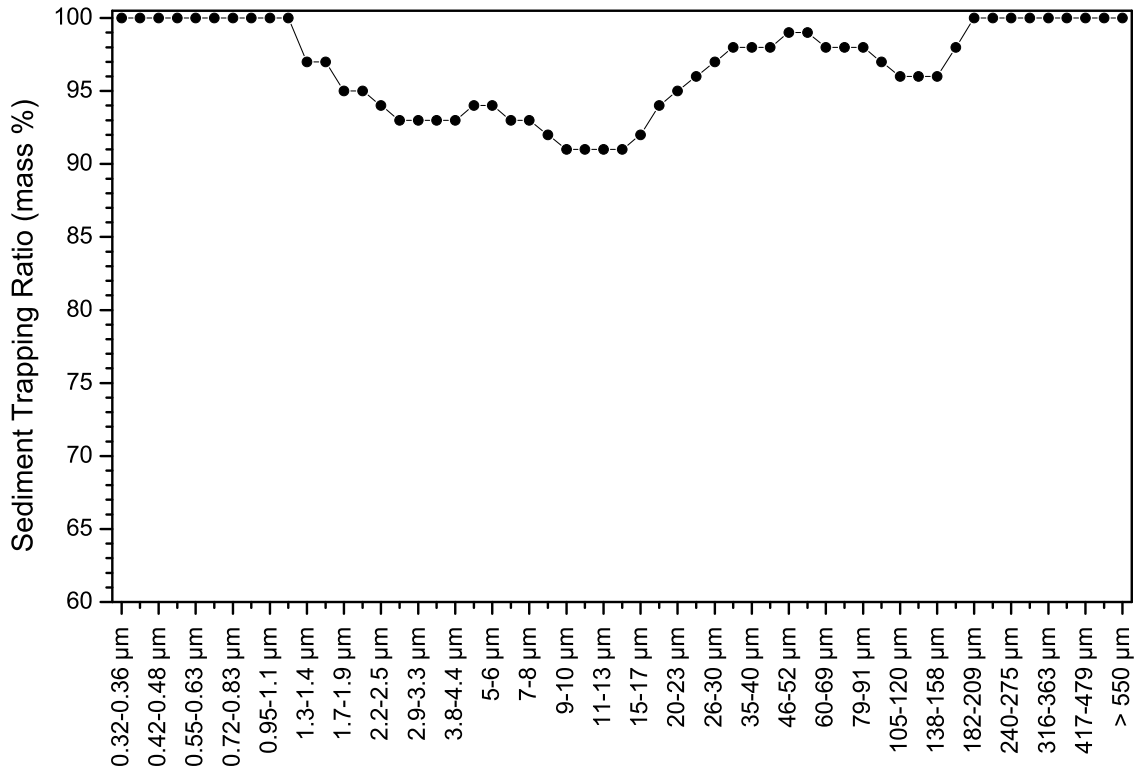


Figure 9: Mineral Soil Fragments budget by size fraction for rainfall event # 2. This budget was computed for a bulk density, $\rho_d(MSF)$, of $2.2 \text{ g}\cdot\text{cm}^{-3}$ measured by [Chepil \(1950\)](#) for silt loam aggregates $< 500 \text{ }\mu\text{m}$.

1 **List of Tables**

2	1	Characteristics of the simulated rainfall events.	44
3	2	Computed hydraulic parameters	45
4	3	Dry and wet bulk densities of the oversize COF	46
5	4	Total sediment exportations and budget	47

Rainfall event	Pre-wetting	# 1	# 2
Duration (min)	13	30	30
Rainfall intensity ($\text{mm}\cdot\text{h}^{-1} \pm \text{SD}$)			
Experimental area	48 ± 22	49 ± 23	75 ± 38
Pasture plot	47 ± 25	50 ± 25	72 ± 43
Pasture + tree belt plot	52 ± 23	49 ± 22	82 ± 40
Median drop size (mm)	1.6	1.6	2.0
ARI (y)	$\simeq 2$	$\simeq 10$	$\simeq 50$

Table 1: Characteristics of the simulated rainfall events.

SD: Standard Deviation. Rainfall intensity was measured with a network of 24 raingauges on the pasture part of the experimental plot.

ARI: Average Recurrence Interval. Data for the determination of the ARI were prepared by the Hydrometeorological Advisory Service, Melbourne, Commonwealth of Australia, Bureau of Meteorology as indicated in [Canterford et al. \(1987\)](#).

Rainfall event	Flow depth		Average flow velocity		Hydraulic roughness	
	mm \pm AME		m·s ⁻¹ \pm AME		<i>n</i>	
	Pasture	Tree belt	Pasture	Tree belt	Pasture	Tree belt
# 1	2.3 \pm 0.3	7.2 \pm 0.5	0.06 \pm 0.01	0.02 \pm 0.00	0.01–0.05	0.12–0.28
# 2	7.5 \pm 2.4	11.3 \pm 2.7	0.04 \pm 0.01	0.03 \pm 0.01	0.03–0.17	0.08–0.24

Table 2: Hydraulic parameters computed by [Ellis et al. \(2006\)](#) from the discharge data. AME: Absolute Measurement Errors. *n* is Manning’s hydraulic roughness.

Fraction	Description	ρ_d g·cm ⁻³	ρ_w g·cm ⁻³
<i>Callistemon</i> spp.	Whole leaves and leaf fragments	0.27	0.59
Round	Mainly small sticks, some small spherical fruits, some grass	0.59	1.15
Flat	Mainly <i>Acacia</i> spp. leaf fragments, some moss	1.03	1.84
Total COF		0.50	0.95

Table 3: Dry and wet bulk densities of the oversize Coarse Organic Fragments.
 ρ_d : dry bulk density; ρ_w : wet bulk density; COF: Coarse Organic Fragments.

Rainfall event	Total mass of sediment exported (kg)			STR
	Pasture	Pasture + tree belt	Tree belt	%
# 1	19.8	0.9	0.01	95
# 2	41.3	2.7	0.35	94
Total	61.1	3.6	0.36	

Table 4: Total sediment exportations and budget.
STR: Sediment Trapping Ratio in mass percentage.